Supramolecular Chemistry
Publication details, including instructions for authors and subscription information:
http://www.informaworld.com/smpp/title~content=t713649759

Expitaxial growth of size-quantized semiconductor particles at monolayers

Janos H. Fendler[a]
[a] Department of Chemistry, Syracuse University Syracuse, New York, USA

To cite this Article Fendler, Janos H.(1995) 'Expitaxial growth of size-quantized semiconductor particles at monolayers', Supramolecular Chemistry, 6: 1, 209 — 216
To link to this Article: DOI: 10.1080/10610279508032536
URL: http://dx.doi.org/10.1080/10610279508032536

SUPRAMOLECULAR CHEMISTRY, Vol. 6, pp. 209–216
Reprints available directly from the publisher
Photocopying permitted by license only

Expitaxial growth of size-quantized semiconductor particles at monolayers

JANOS H. FENDLER

Department of Chemistry, Syracuse University Syracuse, New York 13244-4100 USA

(Received April 19, 1995)

Demonstration of epitaxial lead sulfide (PbS),[1] lead selenide (PbSe),[2] and cadmium sulfide (CdS)[3] growth of semiconductor nanocrystallites under monolayers represents an important milestone in molecular recognition and paves the way for our membrane-mimetic approach to advanced materials synthesis.[4] Oriented growth of semiconductor,[4,5] as well as glycine,[6] sodium chloride,[7] barium sulfate,[8] calcium carbonate,[9] and silver propionate,[10] crystallites under monolayers has, of course, been inspired by biomineralization—the selective crystallization at cell membrane surfaces.[11–13]

Lead sulfide under arachidic-acid monolayers[14]

Lead-sulfide particulate films were formed by exposing a $Pb(NO_3)_2$ solution, coated by an AA monolayer, to hydrogen sulfide gas in a sealed system. The degree of compression was controlled such that the monolayer was in a solid crystalline state. TEM of the crystals showed that they had very regular equilateral triangular morphologies (Figure 1) and that the size of the crystals was highly dependent on the rate of crystal growth. Infusion of H_2S for only 5 minutes yielded crystals with sides of a mean length of 297 Å, while a reaction time of 30 minutes produced significantly larger crystals of a mean side length of 607 Å. Selected area electron diffraction of the crystalline films yielded "single crystal" patterns, indicative of an epitaxial relationship between the PbS particles and the crystalline monolayer. Reciprocal lattice spots corresponding to {220}, {422}, {440}, etc., forms of planes of the cubic PbS structure were identified and demonstrated that all of the crystals nucleated and grew from {111} basal planes. PbS crystals were also grown under monolayers that were maintained at lower surface pressures. Even gaseous state monolayers provided a substrate for the epitaxial growth of PbS. Circular domains of epitaxially oriented PbS particles were located, presumably having grown from crystalline domains of AA which are surrounded by disordered molecules in the gas phase.

The mechanism of oriented crystal growth was rationalized by comparison of the structures of the AA monolayer and the PbS crystals. Synchrotron X-ray studies of AA monolayers in their solid states showed that they comprise fully extended molecules, bearing a planar zig-zag conformation.[15,16] The AA molecules are

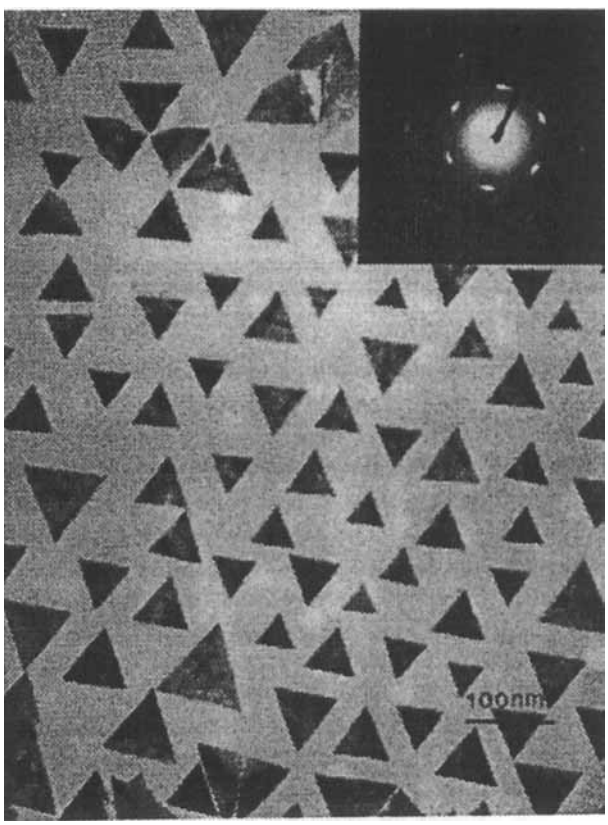

Figure 1 Transmission electron micrograph of a PbS particulate film. The film was formed by the infusion of H_2S to an AA monolayer, floating on an aqueous 5.0×10^{-4} M $Pb(NO_3)_2$ solution in a circular trough, for 45 minutes. The PbS particulate film was deposited on an amorphous-carbon-coated, 200-mesh copper grid. The bar represents 200 nm. Insert: Electron diffraction of a PbS particulate film domain. Limiting aperture was applied to cover an area of 2 μm in diameter.

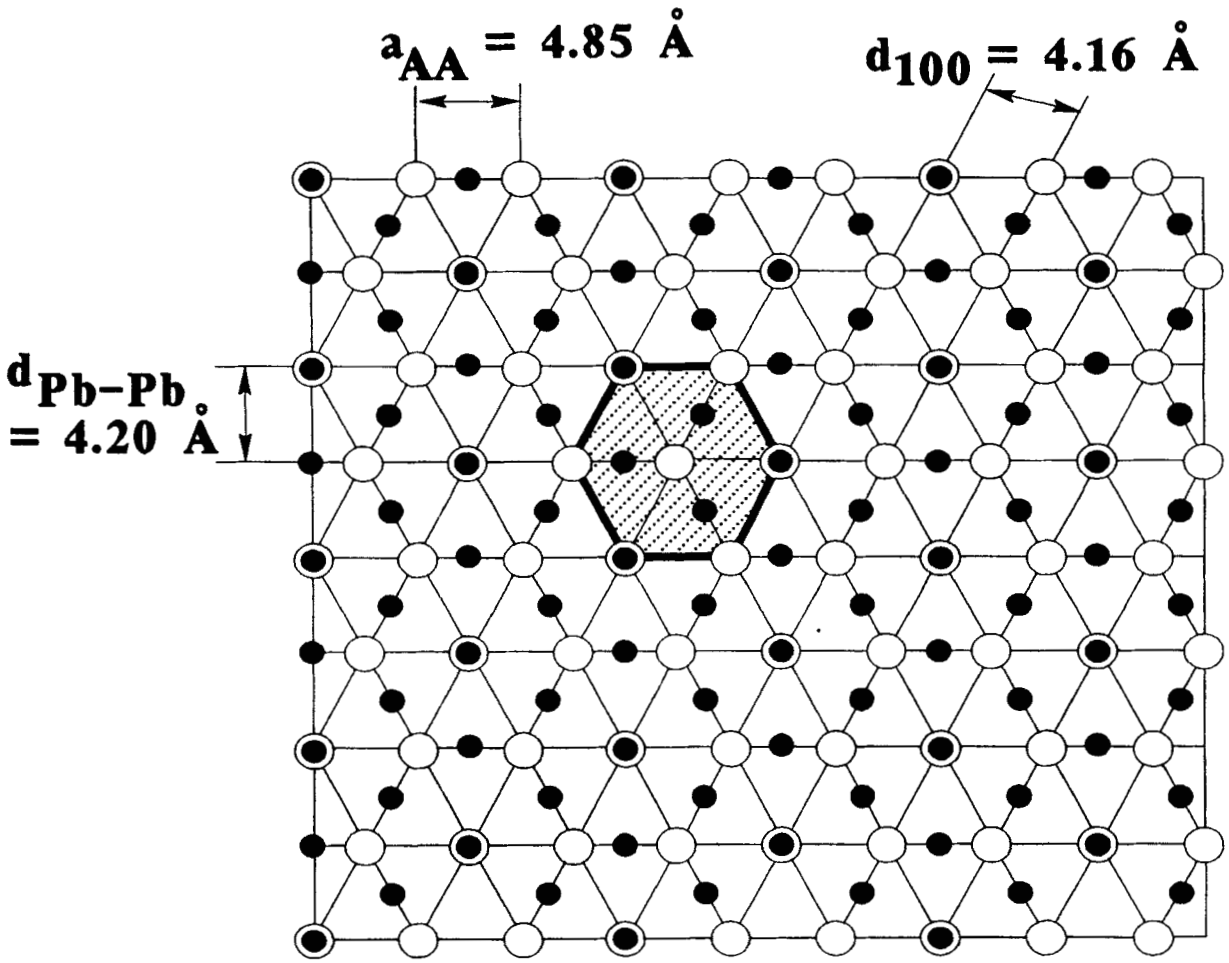

Figure 2 Schematic two-dimensional representation of the proposed overlap between Pb^{2+} ions and AA headgroups; ○ = AA headgroup, ●= Pb^{2+}, and ◉ = Pb^{2+} and AA headgroups. A unit cell is highlighted by the dotted area which is enclosed by heavy lines.

oriented approximately normal to the liquid surface in a hexagonal close-packed array and exhibit a lattice constant of a = 4.85 Å. An experimentally obtained lattice constant of AA monolayers on $Pb(NO_3)_2$ of a = 4.81 Å, as derived from surface pressure *vs.* surface area isotherms, was considered to be in good agreement with the published data and was utilized in the analysis. PbS possesses a NaCl-type cubic structure with a lattice constant of a = 5.9458 Å. Epitaxial growth of PbS from the {111} face resulted from the geometrical complementarity between the AA monolayer and the {111} PbS face (Figure 2). The Pb-Pb and S-S interionic distances of 4.20 Å in the PbS {111} plane geometrically matched the d{100} spacing of 4.16 Å for AA; the spatial mismatch between the crystals is only in the order of 1%.

Lead sulfide growth under mixed arachidic-acid and octadecylamine monolayers[17]

The investigations of epitaxial lead sulfide growth were extended by doping the supporting AA monolayer with octadecylamine (ODA).[18]

The size and orientation preference of lead sulfide grown under mixed AA/ODA monolayers was shown to be profoundly influenced by the AA/ODA ratio and the applied surface pressure. The experimental results are illustrated in Figure 3 and summarized in Table I.[18]

The lead sulfide growth habit was observed to change from [111] to [001] with a reduction in the AA:ODA ratio from 1:0 and 5:1 to 2:1. The II *vs.* A isotherms were identical for these monolayer compositions, indicating a maintenance of the hexagonal close-packed structure.[18]

Epitaxial growth of lead selenide under arachidic-acid monolayers

AA monolayers were also demonstrated to support epitaxial growth of lead selenide crystals.[2] At a surface pressure of 35 mN/m, equilateral triangles with a mean side length of 50.1 nm were precipitated. Selected-area electron diffraction of these crystals gave single-crystal type patterns, showing that the crystals were epitaxially orientated with respect to the monolayer and that they nucleated from {111} basal planes. Increase in the

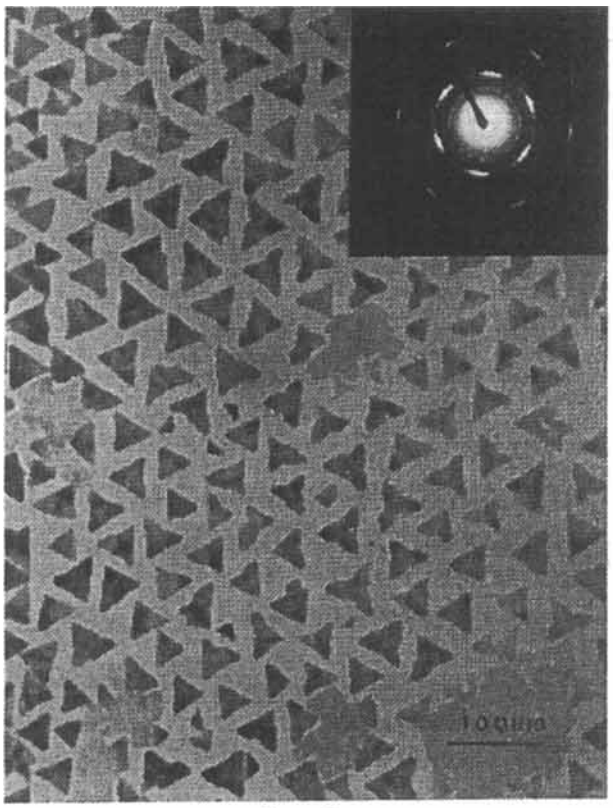

Figure 3a

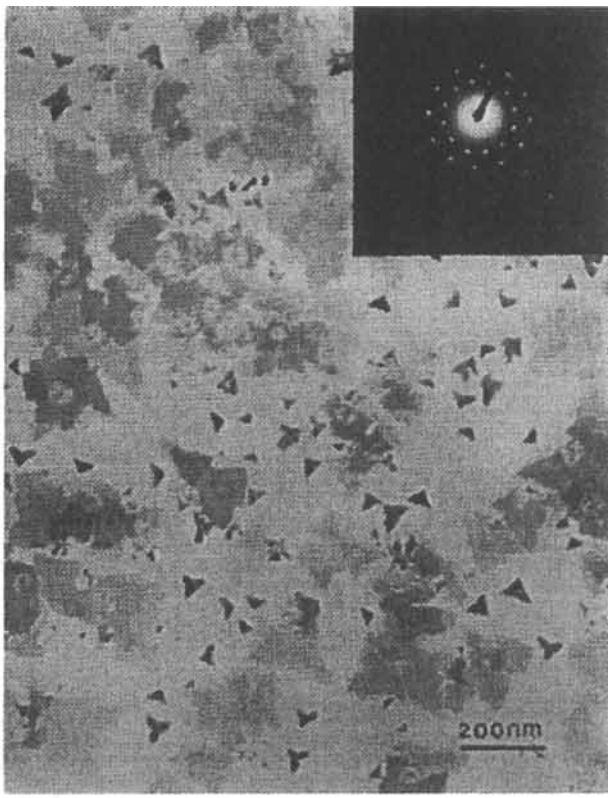

Figure 3b

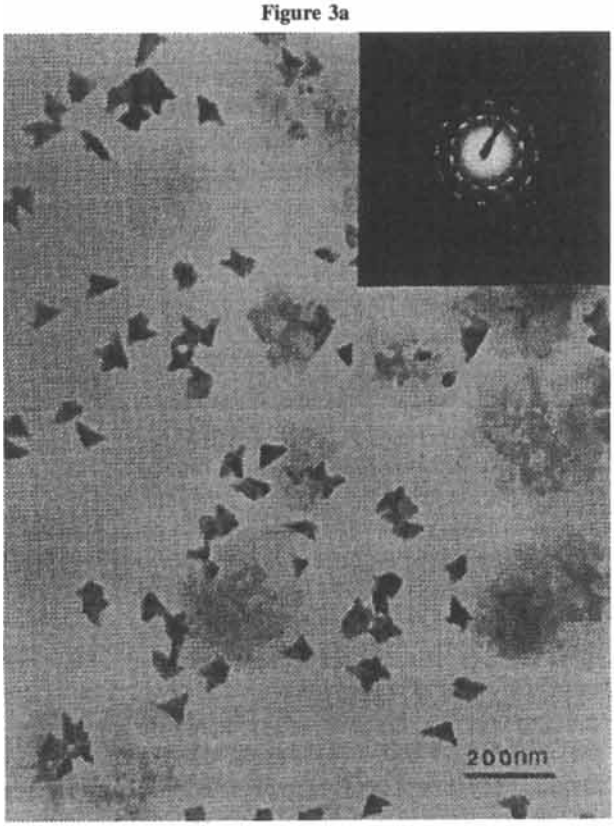

Figure 3c

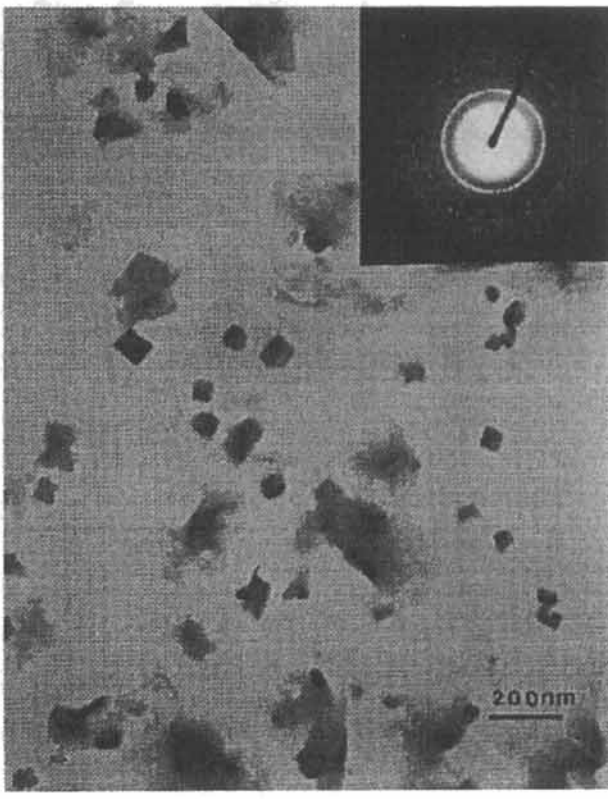

Figure 3d

Figure 3 Transmission electron micrographs and electron diffraction patterns (obtained from 2-μm areas) of PbS nanocrystallites, generated under monolayers prepared from mixtures of AA:ODA = 5:1 (a), AA:ODA = 2:1 (b), AA:ODA = 1:1 (c), and AA:ODA = 1:2 (d), on Formvar-coated 200-mesh copper grids. The monolayers were spread in a Langmuir trough over aqueous 1.0×10^{-3} M $Pb(NO_3)_2$ solutions. PbS nanocrystallites were formed under the monolayers, compressed to Π = 30 mN/m, upon exposure to H_2S. The substrates (Formvar-coated, 200-mesh copper grids) were inserted vertically through the PbS-coated monolayer, turned parallel to it, and then lifted horizontally to effect the transfer. Scale bars = 100 nm (a), 200 nm (b and c), and 250 nm (d).

Table I. PbS nanocrystallites grown under monolayers prepared from AA and ODA mixtures.

AA:ODA[a]	*Diffraction Pattern*	*Orientation Preference*	*Morphology*
1:0	six-fold {220}, {420}, {440}...	epitaxy on {111}	equilateral triangles, 45 ± 9 nm
5:1	same as in the 1:0 case, but dispersed spot	epitaxy on {111}	indented triangles, 45 nm
2:1	twelve-fold {200}, {220}, {400}...	epitaxy on {001}	irregular (100 nm) and some right angular (50 nm)
2:1[b]	six-fold {111}, {200}, {222}, {311}, {400}...	epitaxy on {110}	mostly right-angle triangles
1:1	twelve-fold {200}, {220}, {400}...but spots are dispersed	epitaxy on {001}	mostly right-angle triangles
1:2	powder ring; most {200}, {220}, {400}	no epitaxy; but {001} preferred	square shape (*ca.* 80 nm), sparsely distributed
1:5	NA	NA	crystals grew in bulk solution rather than under monolayers
0:1	NA	NA	crystals grew in bulk solution rather than under monolayers

[a]Surface pressure of the monolayer was kept at 30 mNm, unless stated otherwise.
[b]Surfactant mixture spread in a circular trough, kept at 0 mN/m.

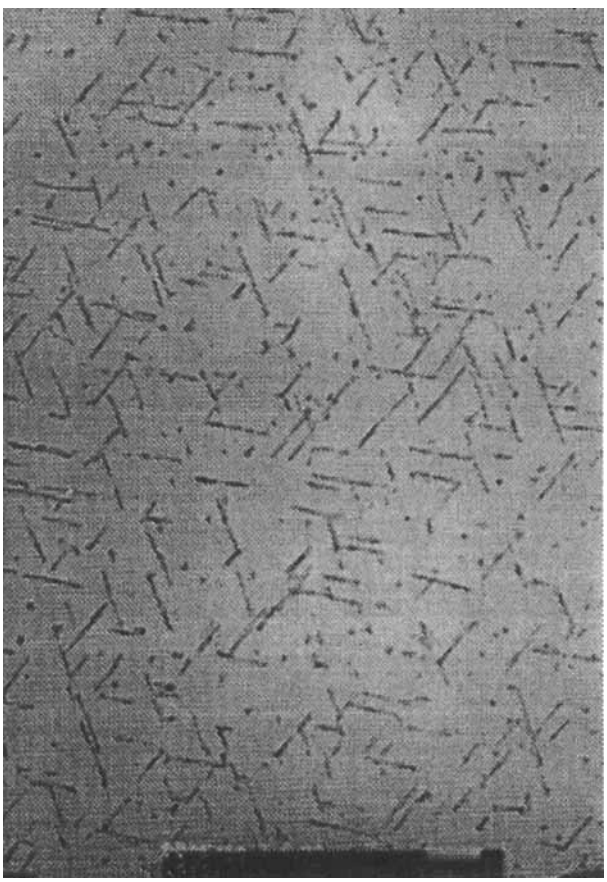

Figure 4 Transmission electron micrograph of a PbSe particulate film. The film was formed by the 25-minute infusion of H_2Se (50 μL) over an AA monolayer, kept at 40 mN/m, which was floating on an aqueous 5.0×10^{-4} M $Pb(NO_3)_2$ solution in the Lauda trough. The PbSe particulate film was transferred to an amorphous-carbon-coated 200-mesh copper grid.

monolayer surface pressure resulted in a dramatic alteration in crystal morphology, with fine, rod-like PbSe particles being produced (Figure 4). The rods were typically 100 nm long and of widths of 10 nm or less. These crystals were shown, by electron diffraction, to be aligned with respect to the monolayers and to exhibit {110} basal planes. Growth from the monolayer on the PbSe {111} face was attributed to a good spatial match between the AA monolayer and this crystal face. PbSe crystallizes with an FCC structure that has a lattice constant of 6.1255 Å. The structure of the AA monolayers on a $Pb(NO_3)_2$ solution was as assumed in the preceding section. A 4% mismatch exists between the d{100} of AA = 4.16 Å and the Pb-Pb separation in the {111} PbSe of 4.33 Å. Rod-like particles, growing from the {110} face, have long and short axes corresponding to the [001] and [1$\bar{1}$0] axes, respectively (Figure 5). Lattice mismatches of 2% and 10% along the [001] and [1$\bar{1}$0] axes favored growth along the [001] axis and resulted in the observed rod-like morphologies.[2]

Crystallization of cadmium sulfide under arachidic-acid monolayers[19]

Epitaxial growth of cadmium sulfide crystals was achieved under AA monolayers, at both room and low temperature, via the slow infusion of hydrogen sulfide gas into the closed environment which surrounded a trough containing a cadmium chloride solution subphase and the AA monolayer.[19] TEM showed that both isolated crystals and areas of densely packed crystals had been precipitated on the monolayer. The crystals were principally rod-like in morphology, with lengths of 50–300 nm

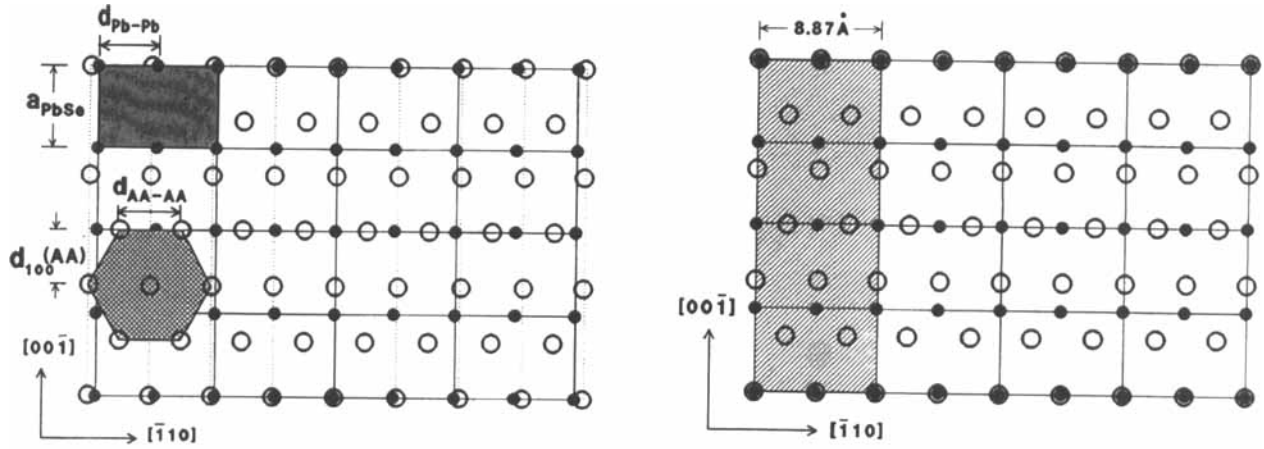

Figure 5 a) Schematic two-dimensional representation of Pb^{2+} (●) in the (110) plane of unstrained lattice (a = 6.125 Å) and hexagonally close-packed AA () headgroups. Two directions are indicated as [00$\bar{1}$] and [$\bar{1}$10] in the PbSe lattice. Both unit cells of AA headgroups and Pb^{2+} ions are highlighted by hexagonal and rectangular shaded areas, respectively. The mismatch between PbSe and AA crystal lattices is evident. b) Schematic two-dimensional representation of the improved matching achieved by stretching PbSe lattice along [$\bar{1}$10] direction. The strained PbSe crystal lattice was experimentally determined as a = 6.27 Å.

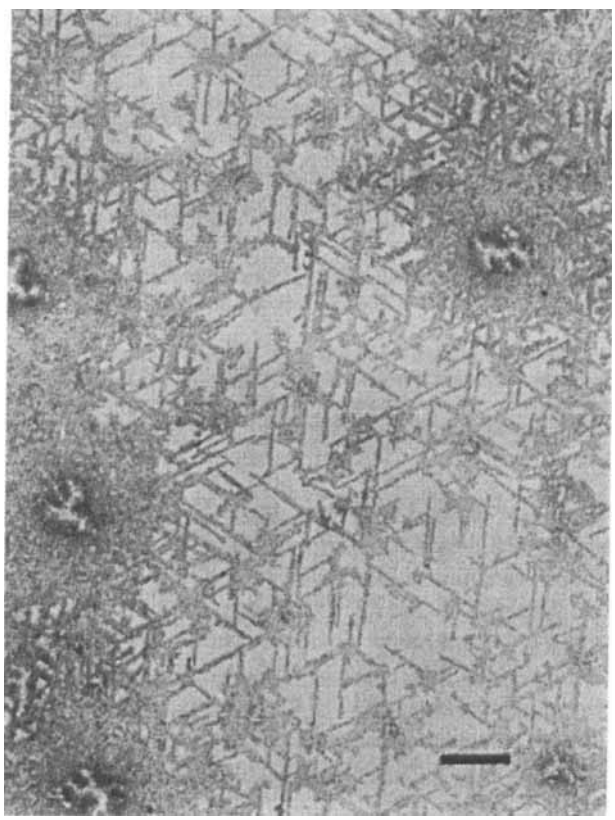

Figure 6 a) Transmission electron micrograph of CdS crystals grown under an AA monolayer at room temperature. Scale bar = 200 nm. b) Selected-area electron diffraction pattern of the sample shown in Figure 6a.

and widths of 5–15 nm, and extensive twinning, apparent as dendritic outgrowths from the main crystal, was present. A smaller proportion of crystals displaying disk-like morphologies was also observed (Figure 6).

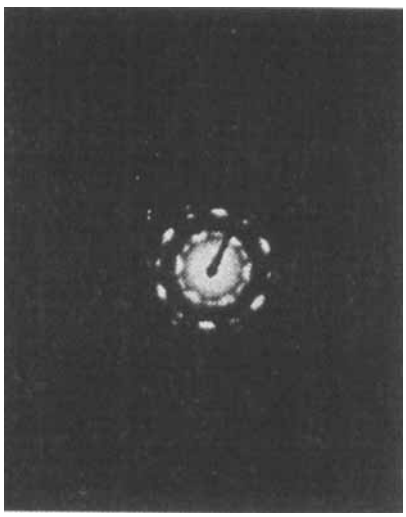

Figure 6b

Conspicuously, the crystals only grew in three directions with respect to the monolayer, these directions being at angular separations of 120°. Selected-area diffraction patterns possessed six-fold geometry and demonstrated that the CdS crystals grew epitaxially with respect to the monolayer. Analysis of the patterns showed that CdS crystals were of hexagonal structure and that nucleation occurred from both the {0001} and the {01.0} faces. CdS can also crystallized by aqueous precipitation as a cubic lattice of zinc-blend structure, but this form is somewhat less common.

Reduction in the temperature of the experiment dramatically decreased the rate of crystallization and yielded thinner crystals. This was supported by a concomitant blue shift in the absorption edge of the crystals from 520 nm to 480 nm upon cooling. A bandgap of 520 nm is characteristic of bulk cadmium sulfide, while a

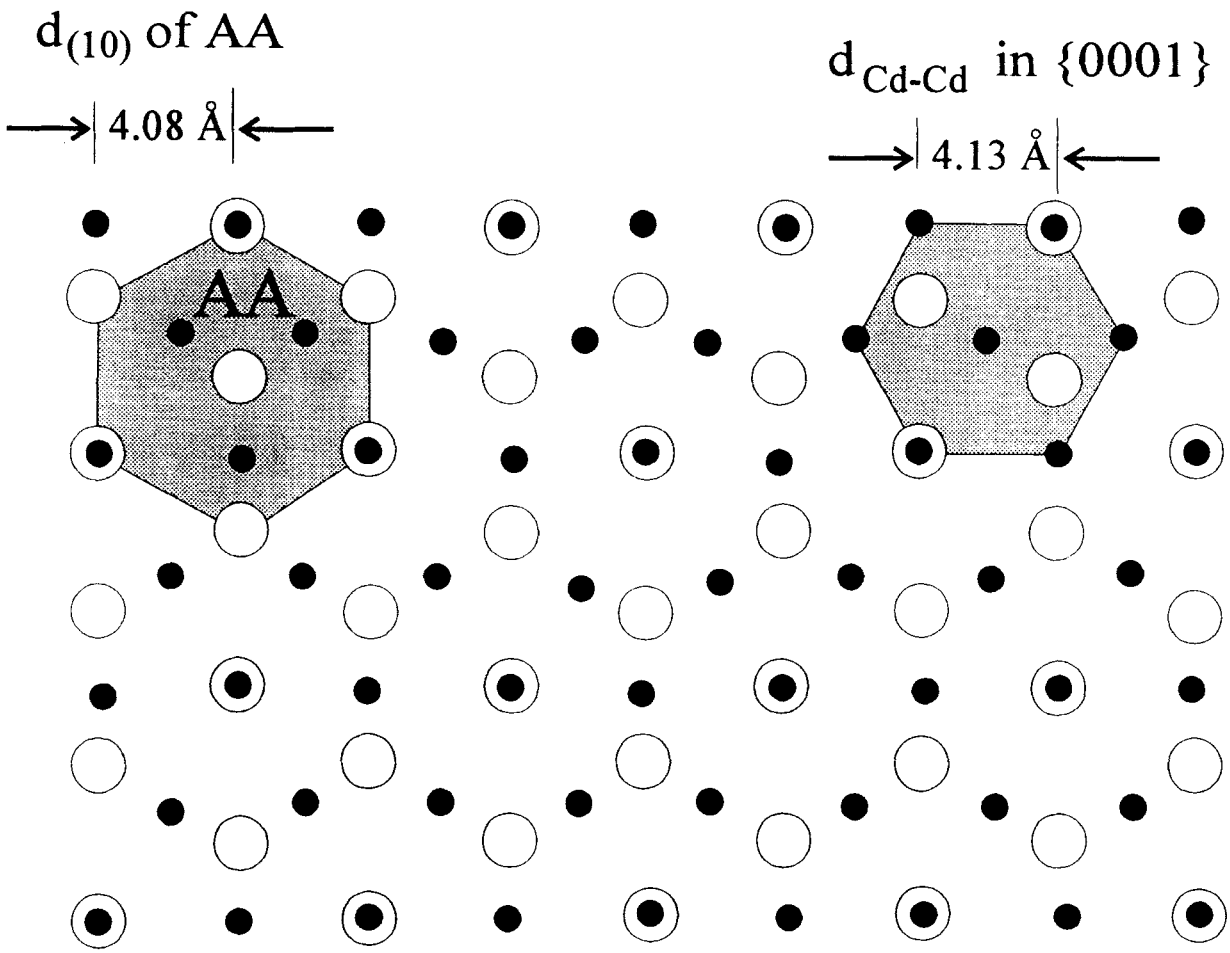

Figure 7 a) Schematic diagrams showing the possible matching between hexagonal close-packed AA headgroups (empty circles) and hexagonal close-packed Cd^{2+} in the {0001} plane (filled circles). The unit cells of both packings are shaded. The calculated d spacing of the {10} plane of AA headgroups (4.08 Å) being equal to the distance between the closest Cd^{2+} cations or $2d_{(11)}$ (4.13 Å) makes such a good matching pattern possible. Bull-eyes represent the positions where AA headgroups and Cd^{2+} cations overlap. Similar matching can be achieved by turning the six-fold AA packing by 60° and 120° without moving the Cd^{2+} packing pattern.

blue-shift to 480 nm is indicative of size quantization and can be correlated with a particle thickness of 38–43 Å.[8b] Electron diffraction of the low temperature CdS yielded very similar patterns to those which were recorded of the room temperature sample.

Consideration of the crystalline structures of the monolayer and the cadmium sulfide particles suggested an epitaxial match between both the {0001} and the {01.0} faces of CdS and the monolayer (Figure 7).[20–22] For the {0001} nucleation face, there is a good lattice match between the arachidic acid head group separation d{10} of 3.98 Å and the Cd^{2+} separation along <100> in CdS of 4.13 Å. The six-fold geometry of the {0001} CdS face thus mimics the structure of the monolayer and it may be anticipated that isotropic crystal growth would occur of this face to produce the disk-like crystals. In the case of the {01.0} nucleation face, a very good correspondence between the lattices in the [10.0] CdS direction exists (d(AA headgroups) along $[\bar{1}1]$ = 3.98 Å and d(Cd-Cd) along [10.0] in CdS = 4.13 Å; only 3.6% mismatch), while the 15% mismatch in the orthogonal [0001] direction is significant (d(AA headgroups) along d[110] = 4.60 Å and d(Cd-Cd) along = 6.75 Å). The final rod-like morphology of the crystals can be directly attributed to this epitaxial relationship. The excellent lattice match along the [10.0] direction results in accelerated growth as compared with that along the [0001] direction where there is significant misfit and associated strain.

CONCLUSION

The epitaxial growth of PbS, PbSe, and CdS nanocrystallites has been realized under surfactant monolayers, floating on aqueous solutions. Importantly, initial observations have suggested marked preparation and morphology-dependent electrical and electro-optical

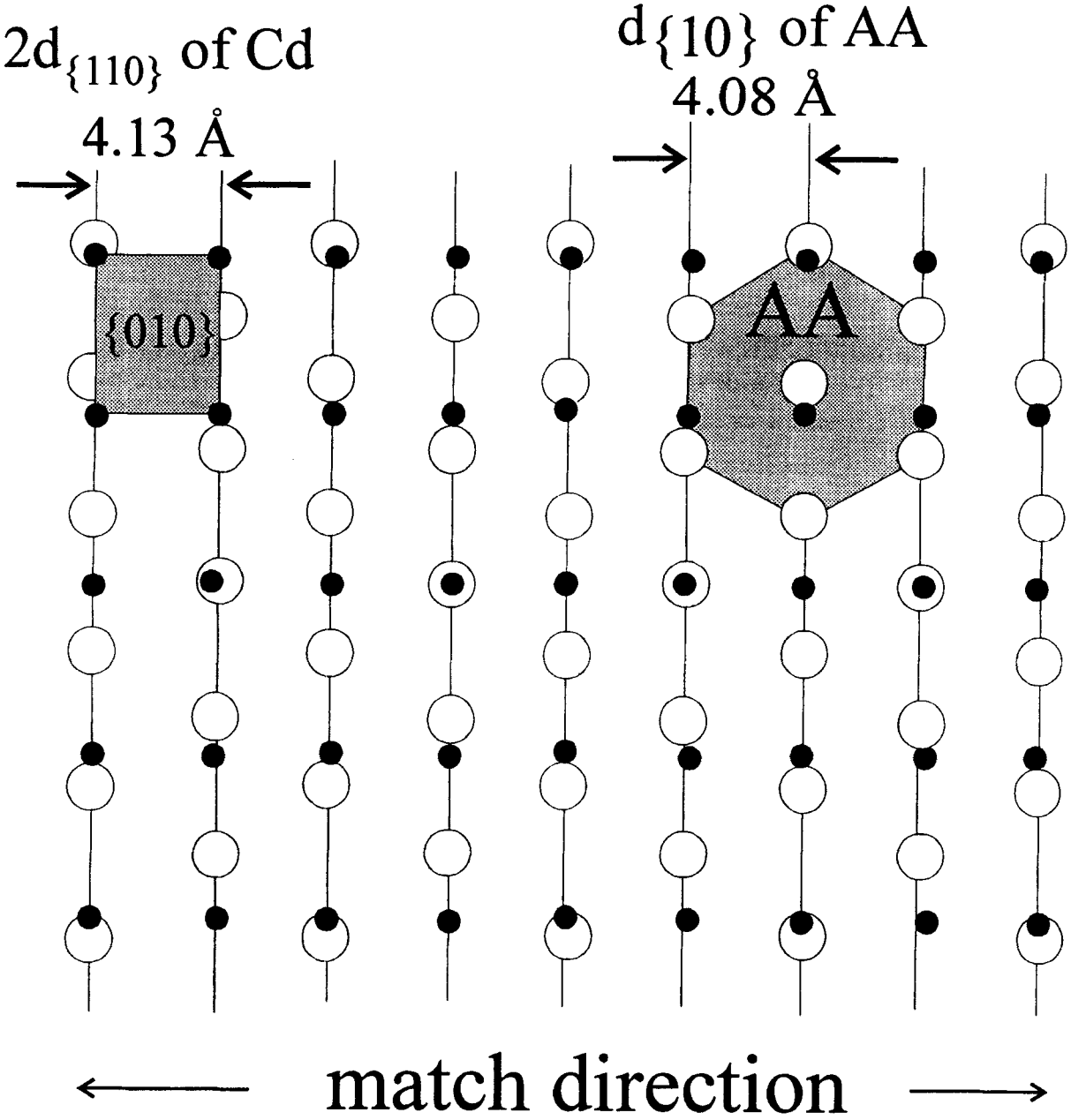

Figure 7 b) Schematic diagrams showing the possible matching along the horizontal direction between hexagonal close-packed AA headgroups (empty circles) and hexagonal close-packed Cd^{2+} in the {0001} plane (filled circles). The unit cells of both packings are shaded. The calculated d spacing of the {10} plane of AA headgroups (4.08 Å) being equal to $2d_{\{11\}}$ of Cd^{2+} cations in the {010} plane (4.13 Å) makes a good match along the horizontal direction. Bull-eyes represent the positions where AA headgroups and Cd^{2+} cations overlap. Similar matching can be achieved by turning the six-fold AA packing by 60° and 120° without moving the Cd^{2+} packing pattern.

properties of the nanoparticulate semiconductor films, generated under monolayers. Taken together, these recent results have already established "wet" colloid-chemical techniques to be a viable alternative approach for the construction of nanostructured materials.

The benefits of a colloid-chemical approach are manifold. The method is relatively simple, convenient to scale-up, inexpensive, and highly versatile. It permits preparation and characterization in solution, at interfaces, and in the solid state, as well as transfers between these phases. This considerably extends the range of possible chemical and physical manipulations and allows characterization at the molecular level with the armory of techniques that are available to chemists. Indeed, the chemical understanding, obtained from initial investigations, has been fueling the construction of new generations of ever more sophisticated nanostructured materials. We can confidently look forward to the development of novel nanostructured devices that are based on imaginative colloid-chemical preparations.

ACKNOWLEDGEMENT

Support of this work by the National Science Foundation (NSF) is gratefully acknowledged.

REFERENCES

1 Zhao, X. K.; McCormick, L. D.; Fendler, J. H. *Adv. Mater.* **1992**, *4*, 93.
2 Yang, J.; Fendler, J. H.; Jao, T.-C.; Laurion, T. *Microsc. Res. Tech.* **1993**, *27*, 402.
3 Yang, J.; Meldrum, F. C.; Fendler, J. H. *J. Phys. Chem.* **1994**, submitted for publication.
4 Fendler, J. H. *Membrane-Mimetic Approach to Advanced Materials*; Advances in Polymer Science Series, Vol. 113; Springer-Verlag: Berlin, 1994.
5 Fendler, J. H.; Meldrum, F. C. *Adv. Mater.* **1994**, submitted for publication.
6 Weissbuch, I.; Addadi, L.; Leiserowtiz, L.; Lahav, M. *J. Am. Chem. Soc.* **1988**, *110*, 561.
7 Landau, E. M.; Popovitz-Biro, R.; Levanon, M.; Leiserowitz, L.; Lahav, M.; Sagiv, J. *Mol. Cryst. Liq. Cryst.* **1986**, *134*, 323.
8 Heywood, B. R.; Mann, S. *Adv. Mater.* **1992**, *4*, 278. Heywood, B. R.; Mann, S. *J. Am. Chem. Soc.* **1992**, *114*, 4681.
9 Heywood, B. R.; Mann, S. *Chem. Mater.* **1994**, *6*, 311.
10 Weissbuch, I.; Majewski, J.; Kjaer, K.; Als-Nielsen, J.; Lahav, M.; Leiserowitz, L. *J. Phys. Chem.* **1993**, *97*, 12848.
11 Mann, S. *Nature* **1993**, *365*, 499.
12 Heywood, B. R.; Mann, S. *Adv. Mater.* **1994**, *6*, 9.
13 Addadi, L.; Weiner, S. *Angew. Chem. Int. Ed. Engl.* **1992**, *31*, 153.
14 Zhao, X. K.; Yang, J.; McCormick, L. D.; Fendler, J. H. *J. Phys. Chem.* **1992**, *96*, 9933.
15 Dutta, P.; Peng, J. B.; Lin, B.; Ketterson, J. B.; Prakash, M.; Georgopoulos, P.; Ehrlich, S. *Phys. Rev. Lett.* **1987**, *58*(21), 2228.
16 Kjaer, K.; Als-Nielsen, J.; Helm, C. A.; Tippmann-Krayer, P.; Möhwald, H. *Thin Solid Films* **1988**, *159*, 17.
17 Phillips, R. J.; Golden, T. D.; Shumsky, M. G.; Switzer, J. A. *J. Electrochem. Soc.* **1994**, *141*, 2391.
18 Yang, J.; Fendler, J. H. *J. Phys. Chem.* **1995**, in press.
19 Yang. J.; Meldrum, F. C.; Fendler, J. H. *J. Phys. Chem.* **1995**, in press
20 Leveiller, F.; Jacquemain, C.; Lahav, M.; Leiserowitz, L.; Deutsch, M.; Kjaer, K.; Als-Nielsen, J. *Science* **1991**, *252*, 1532.
21 Leveiller, F.; Bohm, C.; Jacquemain, D.; Möhwald, H.; Leiserowitz, L.; Kjaer, K.; Als-Nielsen, J. *Langmuir* **1994**, *10*, 819.
22 Andrews, K. W.; Dyson, D. J.; Keown, S. R. *Interpretation of Electron Diffraction Patterns*, Plenum Press, New York **1967**; Wyckoff, R. W. G. *Crystal Structures*, 2nd Ed., Interscience Publishers, New York **1963**.